Carbohydrate Polymers 86 (2011) 1760–1767

Contents lists available at ScienceDirect

Carbohydrate Polymers

journal homepage: www.elsevier.com/locate/carbpol

Facile fabrication of flexible magnetic nanohybrid membrane with amphiphobic surface based on bacterial cellulose

Wen Zhang, Shiyan Chen*, Weili Hu, Bihui Zhou, Zhenhua Yang, Na Yin, Huaping Wang*

State Key Laboratory for Modification of Chemical Fibers and Polymer Materials, Key Laboratory of Textile Science & Technology (Ministry of Education), College of Materials Science and Engineering, Donghua University, Shanghai 201620, PR China

ARTICLE INFO

Article history:
Received 17 May 2011
Received in revised form 1 July 2011
Accepted 9 July 2011
Available online 19 July 2011

Keywords:
Bacterial cellulose
Fe_3O_4 nanoparticle
Magnetic property
Fluoroalkyl silane
Amphiphobicity

ABSTRACT

Flexible magnetic membranes based on bacterial cellulose (BC) with amphiphobicity were prepared firstly by the in situ synthesis of the Fe_3O_4 nanoparticles on the BC nanofibers and then the fluoroalkyl silane (FAS) modification. X-ray diffraction (XRD) patterns indicated the Fe_3O_4 nanoparticles had a spinel structure and field emission scanning electron microscopy (FE-SEM) revealed the Fe_3O_4 nanoparticles were homogeneously deposited on the BC nanofibers. FT-infrared (FTIR) spectra and energy-dispersive spectrum (EDS) demonstrated the presence of FAS. After FAS modification on the magnetic BC membrane prepared by the in situ synthesis of the Fe_3O_4 nanoparticles, the surface wettability of BC membrane was converted from amphiphilicity to amphiphobicity. The fluorinated membrane with appropriate roughness showed the highest water contact angle (WCA) of 130° and oil contact angle (OCA) of 112°. Additionally, the magnetometric measurements revealed that the membranes exhibited the superparamagnetic behavior and can be magnetically actuated. Magnetically responsive BC membrane with hydrophobic and lipophobic surface would have potential applications in electronic actuators, magnetographic printing, information storage, electromagnetic shielding coating and anti-counterfeit.

1. Introduction

Polymer–nanoparticle composites which combine the properties of the polymer and the nanoparticle in a synergistic manner have attracted great attention for the use in various applications. Magnetic nanomaterials have been investigated for biomedical, data storage and device applications (Levison et al., 1998; Zalich, Vadala, Riffle, Saunders, & St. Pierre, 2007; Zhu, Tong, Gao, & Möhwald, 2008). Throughout the literatures, there have been reports of magnetic materials based on cellulose and hydrogels (Liang, Zhang, Jiang, & Li, 2007; Luo, Liu, Zhou, & Zhang, 2009; Small & Johnston, 2009; Sourty, Ryan, & Marchessault, 1998). However, the aggregation problem of magnetic nanoparticles because of the interparticle dipolar forces worsens the properties of the composites and the single function of the magnetic nanomaterials limits their applications. The challenge, therefore, is to inhibit magnetic nanoparticles aggregation and to possess multifunction, without compromising the mechanical properties of the materials (Mackay et al., 2006). Besides that, inexpensive, green and facile processes are also highly desirable.

Unlike the classic mixing of magnetic nanoparticles in a polymer matrix, we propose a new approach using the nanofibril network of bacterial cellulose (BC) as the matrix for the in situ synthesis of the Fe_3O_4 nanoparticles. BC, different from plant cellulose, has attracted great attention due to its high purity (free of hemicellulose, lignin and alien functionalities such as carbonyl or carboxyl groups), the ultrafine network architecture with a distinct tunnel and pore structure, higher specific surface area with a great deal of hydroxyl groups and excellent mechanical strength, etc. (Barud et al., 2011; Huang, Chen, Lin, & Chen, 2011). Additionally, for large-scale production, BC can be easily and inexpensively fabricated by some bacteria species, such as *Gluconacetobacter xylinus* bacteria.

The hydrophilic–lipophilic properties of the BC membrane and its magnetic nanocomposites not only cause dimensional instability but also limit the usage time of the materials. So it is of great importance to fabricate the magnetic nanohybrid membrane with high amphiphobicity.

Amphiphobic surface exhibiting both water and oil repellent properties can generally be fabricated by increasing the surface roughness and decreasing the surface energy of material (Lafuma & Quéré, 2003). The hierarchical roughness at two scale ranges, microroughness and nanoroughness, conduces hydrophobic surface (Jung & Bhushan, 2006; Lafuma & Quéré, 2003). To lower the surface energy, chemicals with low surface energy such as fluorine-based or silicone-based silanes can be used to modify the surface. Fluorinated organic compounds are known to display remarkable hydrophobic–lipophobic properties (Pagliaro & Ciriminna, 2005). The surface modification with fluorinated reagents therefore

* Corresponding authors. Tel.: +86 21 67792958; fax: +86 21 67792726.
E-mail addresses: chensy@dhu.edu.cn (S. Chen), wanghp@dhu.edu.cn (H. Wang).

0144-8617/$ – see front matter.
doi:10.1016/j.carbpol.2011.07.015

represents a promising strategy for the development of materials with novel properties. Fluorinated electrospun inorganic fibrous mats show hydrophobicity such as ZnO (Ding, Ogawa, Kim, Fujimoto, & Shiratori, 2008), SiO_2 (Guo et al., 2010) and Fe_3O_4-filled carbon (Zhu et al., 2006) etc., but the brittleness of inorganic fibrous mats significantly limits their practical application. To the best of our knowledge, there have not been any reports on magnetic material based on bacterial cellulose combined with flexibility and amphiphobic properties. Herein, we attempt to fabricate magnetic BC membrane via in situ synthesis of Fe_3O_4 nanoparticles on the BC nanofibers and then obtain amphiphobic surface by FAS modification. The distribution of Fe_3O_4 nanoparticles is expected to be homogeneous throughout the whole BC membrane. We explore the effects of the ions concentration and attempt to find the optimal reaction conditions. In addition, the surface wettability, the magnetic and mechanical properties of fluorinated membranes are investigated regarding their morphologies and composition.

2. Experimental

2.1. Materials

BC obtained from *Acetobacter xylinum* culture (3 cm × 4 cm × 0.5 cm) was kindly provided by Hainan Yeguo Foods Co. Ltd. $FeCl_2{\cdot}4H_2O$, $FeCl_3{\cdot}6H_2O$ and NaOH were purchased from Aladdin Chemical Company Co., Ltd. Hexane (Junsei) and dodecane (Aladdin Chemical Co., China) were used. FAS ($CF_3(CF_2)_7(CH_2)_2Si(OCH_3)_3$) was purchased from GE Toshiba Silicone Co., Ltd., Japan. Distilled water was used throughout. All reagents were of analytical grade and were used without further purification.

2.2. Fabrication of magnetic membrane

The BC membranes were boiled in 2 wt% NaOH solution and washed with distilled water sufficiently till the filtrate became neutral. The magnetic membranes were fabricated by in situ synthesis as follows. The desired amounts of $FeCl_2{\cdot}4H_2O$ and $FeCl_3{\cdot}6H_2O$ (Fe^{2+} and Fe^{3+} ions in a 1:2 molar ratio) were dissolved in distilled water. The purified BC membrane (3 cm × 4 cm × 0.5 cm) was immersed in the resultant aqueous solution for 12 h. Then, it was taken out and rinsed with distilled water. After that the membrane was immersed in 200 mL of aqueous NaOH (4 mol/L) for 10 min at 60 °C. Nitrogen was bubbled through the whole experiment to prevent Fe^{2+} ions from oxidation. Finally, the membrane was rinsed with distilled water for several times and freeze-dried. The BC membranes treated by the solutions of $FeCl_2{\cdot}4H_2O/FeCl_3{\cdot}6H_2O$ with different concentrations of 1/2, 5/10, 10/20 and 50/100 mmol/L were coded as Fe1, Fe5, Fe10 and Fe50, respectively. And the purified BC membrane without further treatments was coded as Fe0.

2.3. FAS modification

The FAS solution was prepared by dispersing FAS in hexane with a concentration of 3 wt% under stirring strongly for 12 h at room temperature. The prepared samples were immersed into FAS solution for 12 h at room temperature. And then the samples were dried in air. The FAS coated samples of Fe0, Fe1, Fe5, Fe10 and Fe50 were referred to as FS0, FS1, FS5, FS10 and FS50, respectively.

2.4. Characterization

The morphologies of the samples were characterized using S-4800 field emission scanning electron microscope (FE-SEM). Prior to analysis, the samples were cut into small pieces from the prepared samples, and coated with a thin layer of evaporated gold. X-ray diffractometer (XRD) patterns were obtained in a Rigaku D/max-2000 X-ray diffractometer with the Cu Ka radiation ranging from 2 to 80° (2θ angle). The FT-infrared (FTIR) spectra of samples were recorded on a Nicolet NEXUS-670 FTIR. The magnetic properties of the samples were measured with a vibrating sample magnetometer (VSM, Lake Shore 7304, USA). The water contact angle (WCA) and oil contact angle (OCA) of the resultant samples

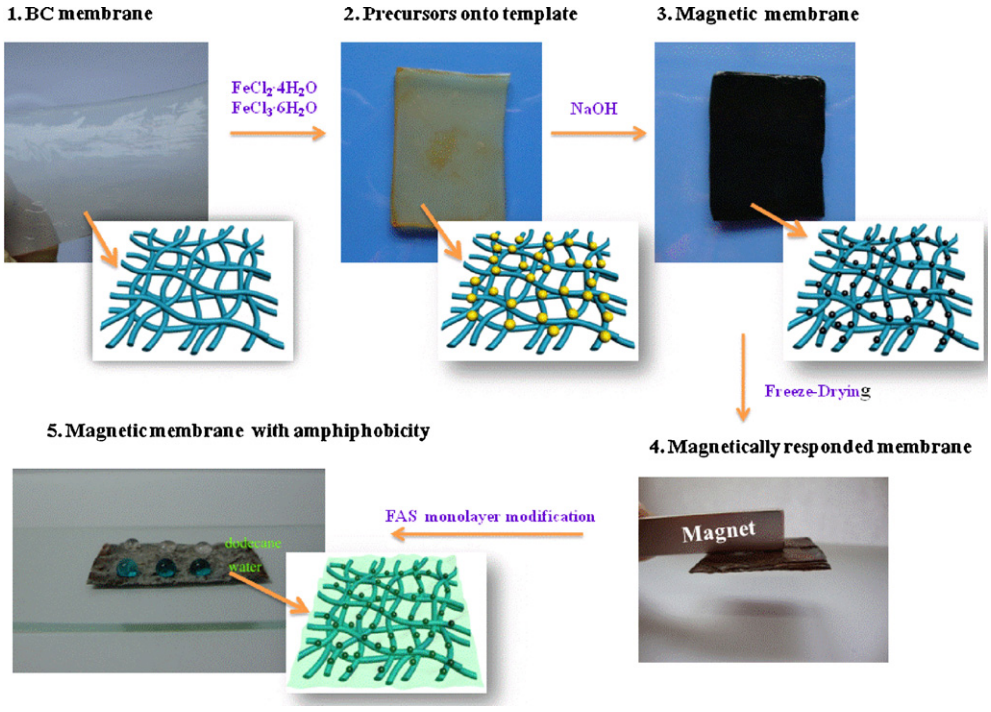

Fig. 1. Schematic illustration for the flexible magnetic nanohybrid membrane with amphiphobic surface.

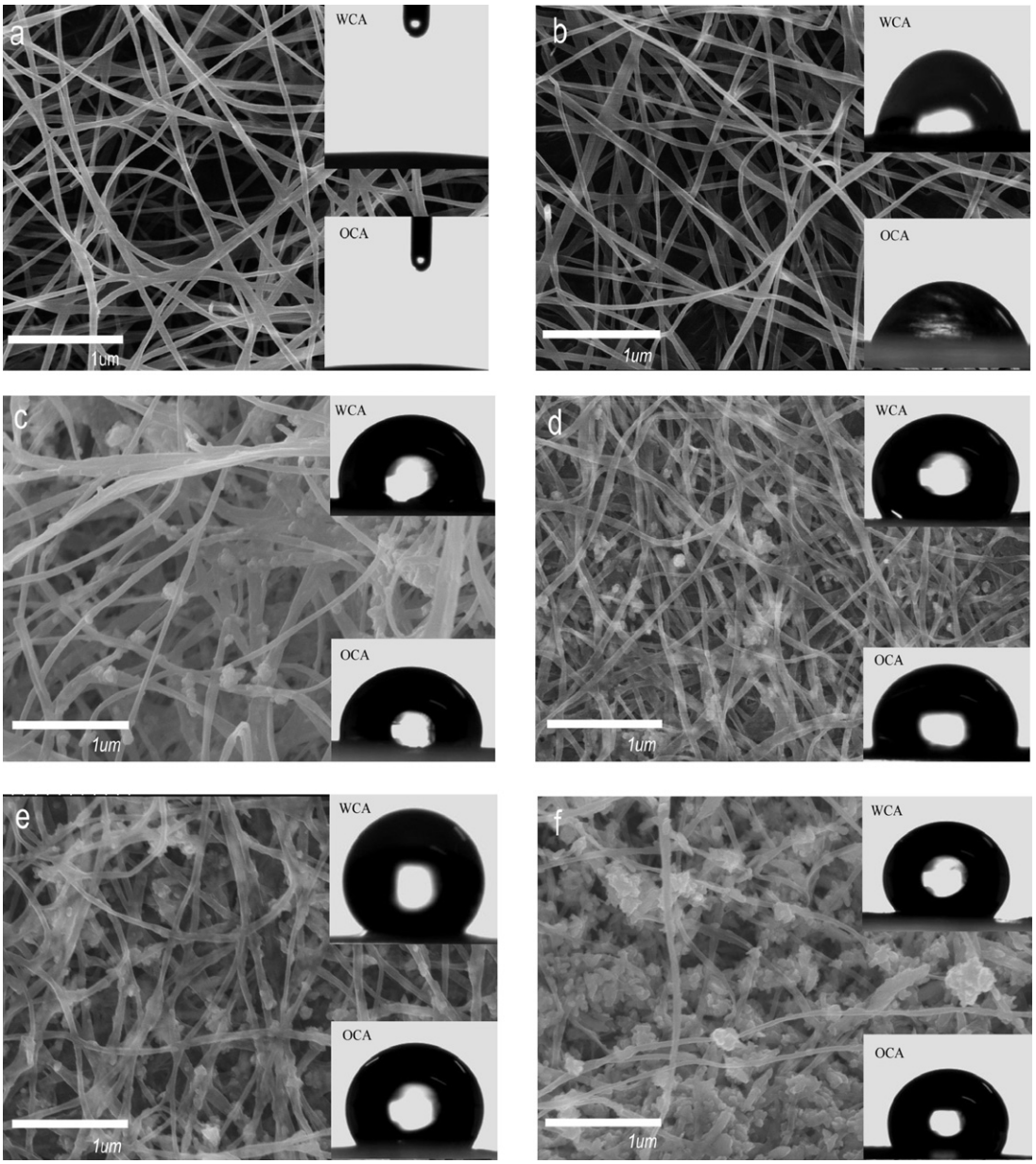

Fig. 2. FE-SEM images of (a) Fe0, (b) FS0, (c) FS1, (d) FS5, (e) FS10 and (f) FS50, respectively. The insets show the profile of water and dodecade droplets on the membrane surfaces.

were measured with a contact angle meter (Contact Angle System OCA40, Dataphysics Co., Germany). Contact angles were measured at six different points of each sample at ambient temperatures. Atomic force microscopy (AFM) images were taken by using the tapping mode of the AFM (Nanoscope IIIa, Digital Instruments). Tensile strengths of the samples were measured using a WDW 3020 Universal Testing Machine at room temperature and a crosshead speed of 10 mm/min. Elongation at break and Young's modulus of these samples were, therefore, measured. Samples with 30 mm in length, 5 mm in width and 0.03 mm in thickness were used in the measurements.

3. Results and discussion

3.1. Synthesis of flexible magnetic nanohybrid membrane with amphiphobic surface

The ultrafine network architecture of BC gives a good tunnel for Fe^{2+}/Fe^{3+} adsorption. Fe^{2+} and Fe^{3+} ions are firstly anchored on some BC nanofibers through ion–dipole interactions (Shim et al., 2002) during the soaking of BC in the solution. The electro-rich oxygen atoms of polar hydroxyl and ether groups of cellulose are expected to interact with electro-positive transition mental cations (Hu et al., 2009; Maneerung, Tokura, & Rujiravanit, 2008). After being rinsed with distilled water to remove the unanchored Fe^{2+} and Fe^{3+} ions, the obtained Fe^{2+}/Fe^{3+}/BC complexes are immersed into the excessive NaOH solution. The interaction between Fe^{2+}/Fe^{3+} and OH^- is immediately seen from the appearance of dark color, as described in Eq. (1). BC serves as an excellent matrix in the in situ synthesis of the Fe_3O_4 nanoparticles.

$$Fe^{2+} + 2Fe^{3+} + 8OH^- = Fe_3O_4 + 4H_2O \quad (1)$$

Reactive alkysilanes are anchored to hydroxyl-bearing groups on the surfaces, such as silica, glass and metal oxide, by a cross-linked siloxane network resulting in the formation of self-assembled monolayers (SAMs) (Fadeev & McCarthy, 2000; Hozumi, Ushiyama, Sugimura, & Takai, 1999; Song, Zhai, Wang, & Jiang, 2006). In the present experiment, modification of FAS is performed

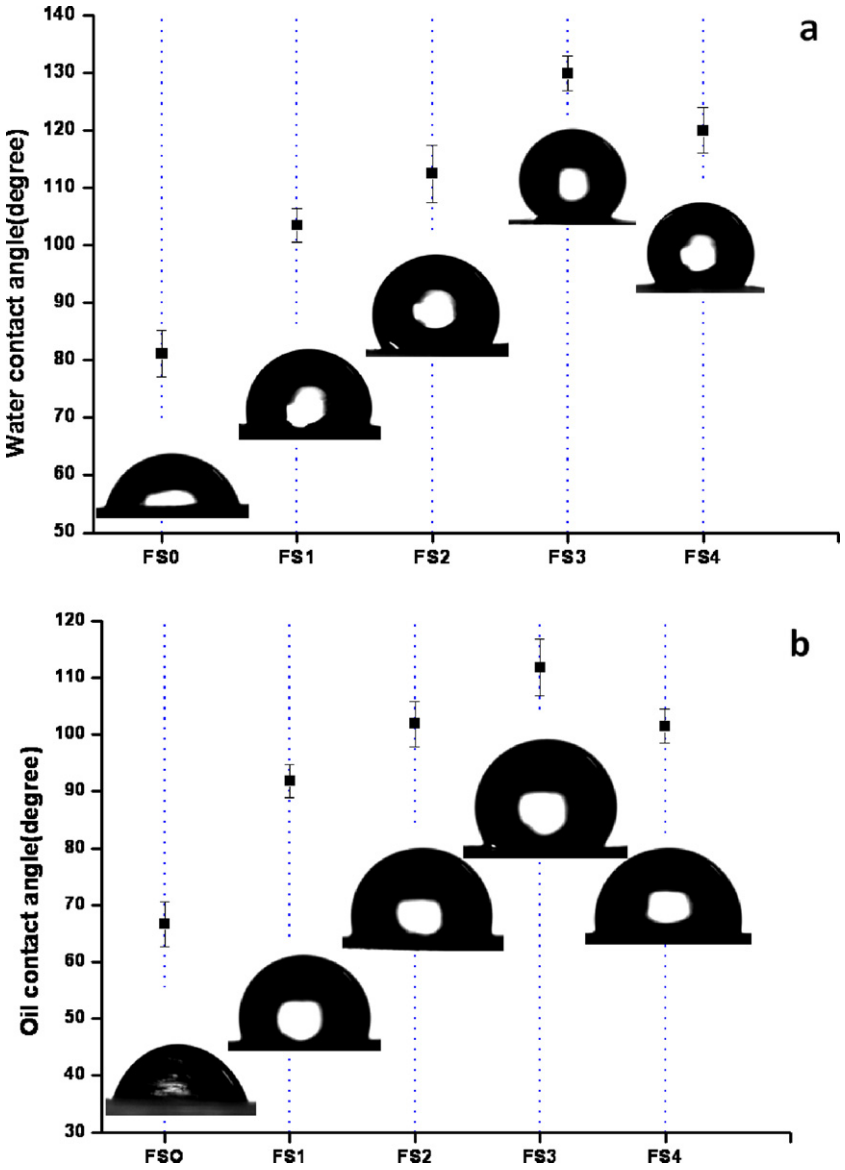

Fig. 3. (a) Water contact angles of the FAS modified samples and the corresponding shapes of water droplets for fluorinated samples; (b) Oil contact angles of the FAS modified samples and the corresponding shapes of dodecane droplets for fluorinated samples.

at the FAS solution/BC membrane interface. FAS is expected to anchored to some hydroxyl groups on the magnetic BC membrane by a cross-linked siloxane network. Fluorinated silane is known to display remarkable hydrophobic–lipophobic properties. So the wettability of the surface is tailored from amphiphilicity to amphiphobicity with the combination of FAS modification and surface roughening. Fig. 1 gives a schematic illustration for the formation process.

3.2. Morphology of the samples and the surface wettability

Fig. 2a shows the 3D porous network structure of Fe0 and the diameters of its nanofibers are around 80 nm. After placing a water or dodecane droplet on it, the droplet is immediately absorbed by this membrane because of the large numbers of hydrophilic hydroxyl groups in BC. The Fe0 shows a WCA of 10° and an OCA of 21°. And Fe1, Fe5, Fe10 and Fe50 show the average WCAs of 20°, 25°, 30°, 38° and average OCAs of 25°, 33°, 39°, 41°, which still demonstrate amphiphilicity. After immersing Fe0 in FAS solution, the fibers' shape and its 3D porous network structure are still maintained (Fig. 2b). However, FS0 shows a WCA of 81° higher than that (10°) of Fe0 and an OCA of 67° higher than that (21°) of Fe0. Water wetting images of FS0, FS1, FS5, FS10 and FS50 at equilibrium are shown in Fig. 3a. The average WCAs of FS0, FS1, FS5, FS10 and FS50 are 81°, 103°, 112°, 130° and 120°, respectively. FS10 shows the highest hydrophobicity among the five samples. Fig. 3b presents the OCAs of FS0, FS1, FS5, FS10 and FS50. The oleophobicity of the samples shows a tendency similar to the hydrophobicity of the samples. And FS10 also shows the highest oleophobicity. Fig. S1a shows the energy-dispersive spectrum (EDS) of Fe10. There are Fe and O elements in the magnetic nanohybrid membrane, which further indicates the Fe_3O_4 nanoparticles have been fabricated successfully by the in situ synthesis. Compared with the EDS of Fe10, the EDS of FS10 (Fig. S1b) shows the existence of F and Si elements, testifying the existence of FAS in FS10. The wettability of the surface is converted from amphiphilicity to amphiphobicity after the modification with FAS. Fig. 2c–f show the FE-SEM images of FS1, FS5, FS10 and FS50, respectively. It can be seen in the pictures that the Fe_3O_4 nanoparticles are synthesized in situ on the BC nanofibers. The morphology and size distribution of the Fe_3O_4 nanoparticles in

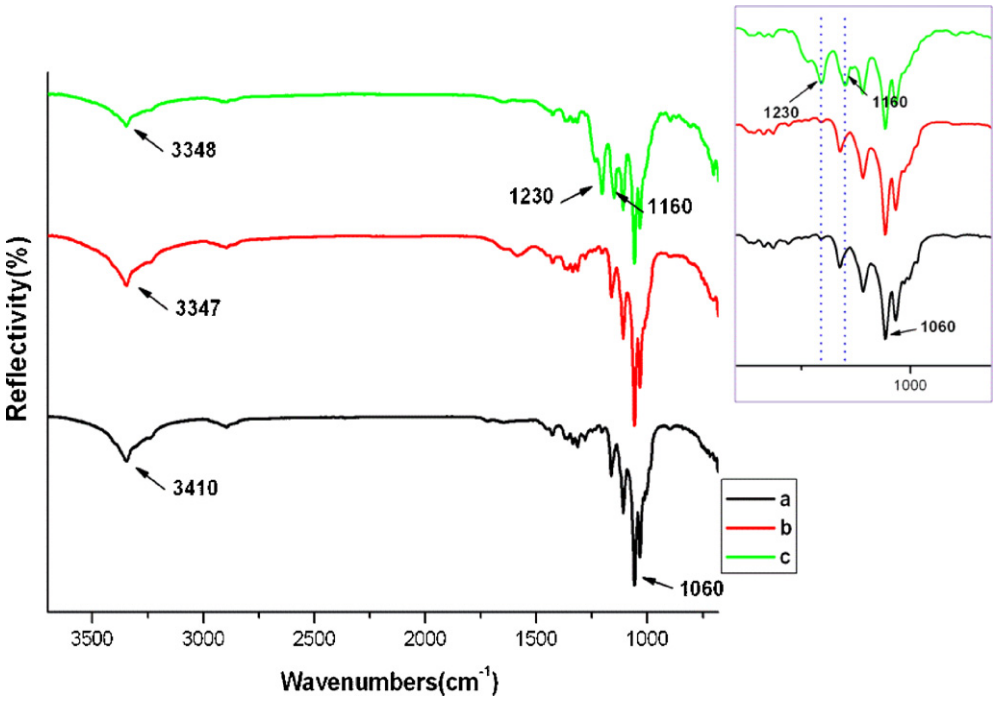

Fig. 4. FTIR–ATR spectra of (a) Fe0, (b) Fe10 and (c) FS10. The inset is the magnification of the FTIR–ATR spectra between 800 cm^{-1} and 1400 cm^{-1}.

FS10 (Fig. 2e) is better than the others. The diameter of the fibers is between 60 and 100 nm and the micro- and nanosized Fe_3O_4 are homogeneously dispersed on the fibers. Proper roughness can enhance hydrophobicity of a solid surface leading to high contact angles with water (Michael & Bhushan, 2007). The formation of the hierarchical micronanostructure results in a thick air layer, which keeps the water and dodecane droplets from contacting with the fibers (Tang, Wang, & He, 2009). The hierarchical micronanostructure of micro- and nanosized Fe_3O_4 deposited on the fibers with the diameter of 80–100 nm in FS10 appropriately increases its surface roughness, which leads to its highest amphiphobicity. With the increased content of iron ions, the Fe_3O_4 nanoparticles tend to agglomerate, as shown in Fig. 2f. Therefore, the proper increase of the surface roughness would be the key parameter to influence the surface wettability when the surfaces have the same chemical composition.

3.3. FTIR–ATR spectroscopy

The FTIR–ATR spectra of Fe0, Fe10 and FS10 are shown in Fig. 4. The characteristic band of BC at around 1060 cm^{-1} corresponding to C–O–C stretching appears in all the samples. However, the peak at 3410 cm^{-1} corresponding to stretching vibrations of hydroxyl groups of BC moves to lower wavenumbers (3348 cm^{-1}), which indicates that the hydroxyl groups have a strong interaction with Fe^{2+} and Fe^{3+} (Li et al., 2009). The occurrence of new bands at 1160 cm^{-1} and 1230 cm^{-1} in FS10, typical of C–F stretching modes, provides additional evidence of the presence of FAS (Cunha, Freire, Silvestre, Neto, & Gandini, 2006; Cunha et al., 2007).

3.4. XRD analysis

Fig. 5 shows the XRD patterns of FS0, FS1, FS5, FS10 and FS50. The broad diffraction peaks at about 14.6° and 22.8° in the XRD pattern of FS0 are assigned to the crystallographic plane of $(1\bar{1}0)$ and (200) reflection of BC (Tokoh, Takabe, Fujita, & Saiki, 1998). The characteristic peaks of the resultant iron oxide nanoparticles at 30.1°, 35.5°, 43.1°, 53.4°, 57.0° and 62.9°, marked by their corresponding indices (220), (311), (400), (422), (511) and (440), are observed in FS1, FS5, FS10 and FS50. Due to the low content of the Fe_3O_4 nanoparticles, the characteristic peaks are not obvious in XRD pattern of FS1. And these peaks are consistent with those reported by Liang et al. (2007) for pure Fe_3O_4 nanoparticles with a spinel structure.

3.5. Surface roughness of BC and FAS modified membranes

It is well known that the surface roughness is the key parameter to influence the surface hydrophobicity when the surfaces have the similar chemical compositions (Miwa, Nakajima, Fujishima, Hashimoto, & Watanabe, 2000). The AFM top view images of Fe0, FS0, FS1, FS5, FS10 and FS50 are shown in Fig. 6, respectively.

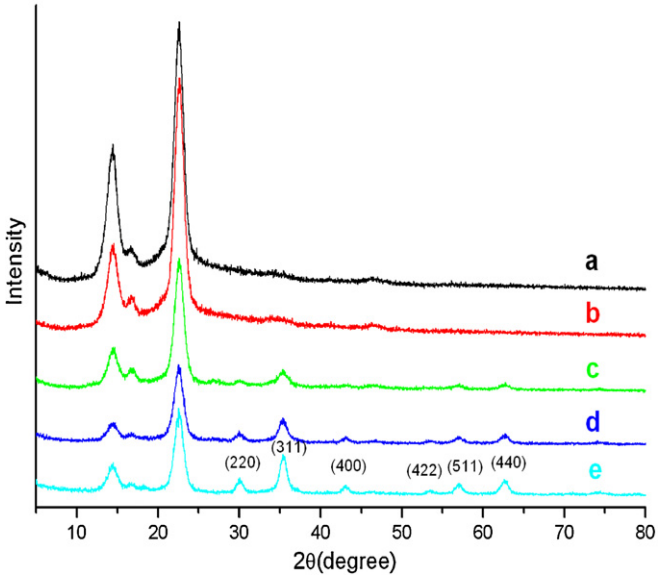

Fig. 5. XRD patterns of (a) FS0, (b) FS1, (c) FS5, (d) FS10 and (e) FS50.

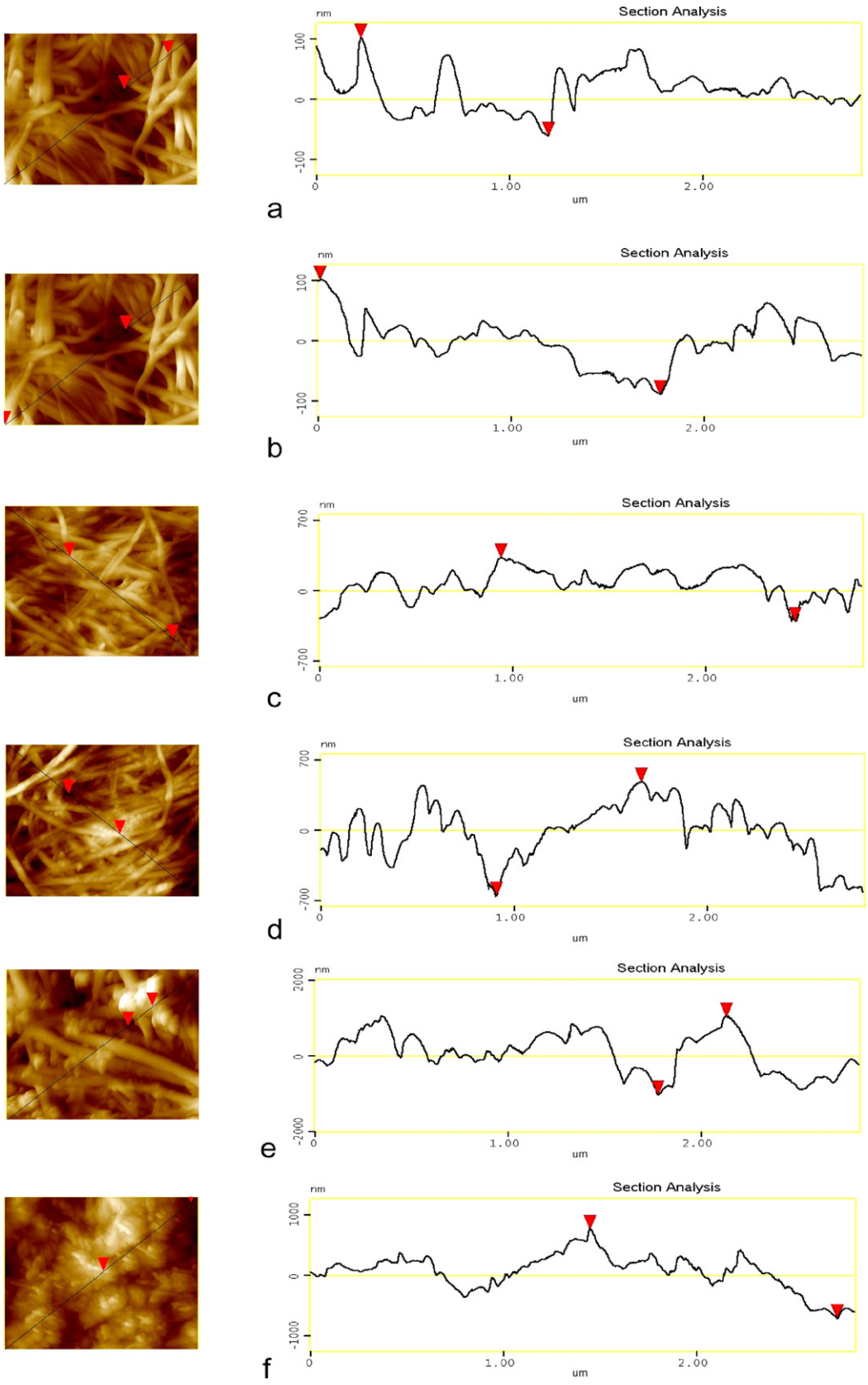

Fig. 6. AFM top view images and cross section profiles along the marked direction of (a) FE0, (b) FS0, (c) FS1, (d) FS5, (e) FS10 and (f) FS50, respectively.

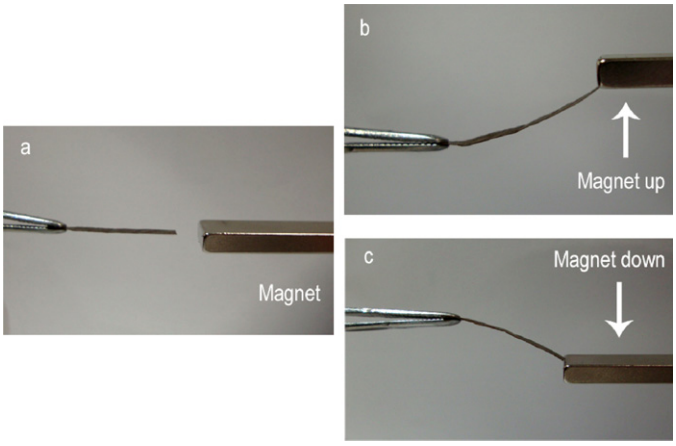

Fig. 7. The picture of magnetically actuated FS10.

The images of Fe0 (Fig. 6a) and FS0 (Fig. 6b) both show relatively smooth fiber surface with the calculated RMS roughness of 61 nm and 75 nm, which identify the FAS modification does not change the surface roughness. The nano-sized particles can be observed in all the AFM top view images of FS1, FS5, FS10 and FS50. Owing to the Fe_3O_4 nanoparticles, the top surface layer of the four samples are not so smooth as Fe0 and Fs0. FS10 (Fig. 6e) shows the RMS roughness of 627 nm, which is identical to the corresponding FE-SEM image (Fig. 2e). As a result, the higher hydrophobicity can be obtained by increasing the surface roughness.

3.6. Magnetic property

Fig. 7 shows that FS10 can be magnetically actuated. When the magnet goes up, FS10 bends towards to the magnet immediately; when the magnet goes down, FS10 follows the magnet (Fig. 7b and c). Our findings suggest that the flexible magnetic nanohybrid membranes possessing a sensitive magnetic response may be used in conditions similar to electronic devices as the sensor and its amphiphobic surface may prolong the usage time as well as to save costs and time for maintenance.

Fig. 8a illustrates the plots of magnetization versus magnetic field at 25 °C for the four samples. Although the magnetization of the Fe_3O_4 nanoparticles in each sample is weak, they exhibit an extremely small hysteresis loop and low coercivity. The lack of hysteresis and coercivity is a characteristic of superparamagnetic particles or some single-domain particles (Leslie-Pelecky & Rieke, 1996; Zhou et al., 2009). The saturation magnetization (M_s) of the membranes is in the range of 1.49–13.67 emu/g, which are related to the increasing content of Fe_3O_4 nanoparticles. Although the magnetic property of FS50 (M_s = 13.68 emu/g) is better than that of FS10 (M_s = 8.03 emu/g) as shown in Fig. 8a, the surface amphiphobicity of FS50 decreases because of the agglomeration of the Fe_3O_4 nanoparticles shown in Fig. 2f. Fig. 8b shows the magnetic hysteresis loops of Fe10 and FS10 at 25 °C. The magnetic hysteresis loop of FS10 coincides with that of Fe10, which indicates the FAS modification does not affect its magnetic property. Table S1 shows the characteristics of the resultant samples.

3.7. Mechanical properties

The tensile behaviors of Fe0, FS0, FS1, FS5, FS10 and FS50 are shown in Fig. S2. The Young's modulus (18.0 GPa) and tensile strength (325 MPa) of FAS modified BC membrane is a little higher than the values of Young's modulus (13.9 GPa) and tensile strength (305 MPa) of BC, which shows the FAS modification does not affect its mechanical properties too much. It is found that the Young's

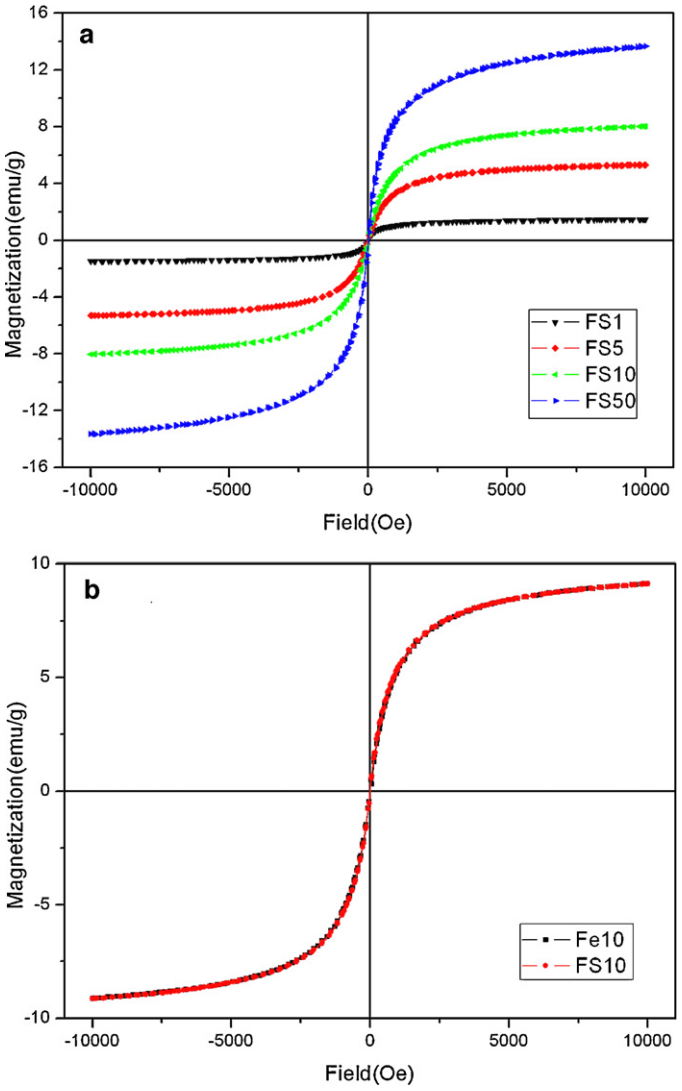

Fig. 8. The magnetic hysteresis loops of (a) FS1, FS5, FS10 and FS50 and (b) Fe10 and FS10 at 25 °C.

modulus and tensile strength of the FS1, FS5, FS10 and FS50 are lower than that of BC due to the lower degree of crystallinity and the less dense network structure. However, with the increased content of the Fe_3O_4 nanoparticles in the membranes, the tensile strength is firstly enhanced and then reduced. FS10 shows the highest tensile strength (186 MPa), which demonstrates the inorganic nanoparticles contribute to the tensile strength of nanocomposites as the enhancer. But when the content of the Fe_3O_4 nanoparticles is further increased, the Young's modulus and tensile strength of FS50 fall due to the agglomeration and fragility of the Fe_3O_4 nanoparticles. Table S2 shows the mechanical properties of the samples.

Fig. S3 demonstrates the striking flexibility of FS10. Repeated bending through 90° and 360° still causes no apparent damage. The present flexibility can be explained by the strong (Yano et al., 2005) and highly entangled nanofibrils of BC substrate, which have lateral dimensions of tens of nanometres and lengths of several micrometres. Previously, magnetic nanoparticle-containing solvent-swollen ferrogels (Bonini, Lenz, Giorgi, & Baglioni, 2007; Fuhrer, Athanassiou, Luechinger, & Stark, 2009; Zrínyi, Barsi & Büki, 1997) have been demonstrated to be responsive materials and actuators. However, drying of such gels and inorganic fibrous mats (Zhu et al., 2006) typically makes the materials brittle. Our findings suggest that this magnetic nanohybrid membranes based on bacterial

cellulose have outstanding flexibility, which greatly expands its application fields.

4. Conclusion

In summary, we have successfully prepared flexible magnetic nanohybrid membrane with amphiphobic surface based on bacterial cellulose simply by in situ synthesis of Fe_3O_4 nanoparticles and FAS modification under moderate condition. The ultrafine network architecture and the ether and hydroxyl groups of BC nanofibers constitute an effective nanoreactor for the formation of Fe_3O_4 nanoparticles. FS10 with the Fe_3O_4 nanoparticles dispersed homogenerously on the BC nanofibers shows the highest amphiphobicity with a WCA of 130° and an OCA of 112° and also demonstrates the superparamagnetic behavior with the M_S of 8.03 emu/g. In addition, FS10 demonstrates the highest tensile strength (186 MPa) among the fluorinated magnetic membranes and outstanding flexibility. This study opens an effective way to fabricate the flexible and magnetic BC membranes with self-cleaning properties. Further investigation such as the influence of different concentration of FAS and immersing time in FAS on the properties of the nanocomposites is in progress.

Acknowledgements

This work was financially supported by Doctoral Fund of Ministry of Education of China (20090075120011), Program of Introducing Talents of Discipline to Universities (B07024), Shanghai Leading Academic Discipline Project (B603), The National Natural Science Foundation of China (51003012), and Project of the Action on Scientists and Engineers to Serve Enterprises (2009GJE20016).

Appendix A. Supplementary data

Supplementary data associated with this article can be found, in the online version, at doi:10.1016/j.carbpol.2011.07.015.

References

Barud, H. S., Souza, J. L., Santos, D. B., Crespi, M. S., Ribeiro, C. A., Messaddeq, Y., et al. (2011). Bacterial cellulose/poly(3-hydroxybutyrate) composite membranes. *Carbohydrate Polymers*, *83*(3), 1279–1284.

Bonini, M., Lenz, S., Giorgi, R., & Baglioni, P. (2007). Nanomagnetic sponges for the cleaning of works of art. *Langmuir*, *23*(17), 8681–8685.

Cunha, A. G., Freire, C. S. R., Silvestre, A. J. D., Neto, C. P., & Gandini, A. (2006). Reversible hydrophobization and lipophobization of cellulose fibers via trifluoroacetylation. *Journal of Colloid and Interface Science*, *301*(1), 333–336.

Cunha, A. G., Freire, C. S. R., Silvestre, A. J. D., Neto, C. P., Gandini, A., Orblin, E., et al. (2007). Characterization and evaluation of the hydrolytic stability of trifluoroacetylated cellulose fibers. *Journal of Colloid and Interface Science*, *316*(2), 360–366.

Ding, B., Ogawa, T., Kim, J., Fujimoto, K., & Shiratori, S. (2008). Fabrication of a superhydrophobic nanofibrous zinc oxide film surface by electrospinning. *Thin Solid Films*, *516*(9), 2495–2501.

Fadeev, A. Y., & McCarthy, T. J. (2000). Self-assembly is not the only reaction possible between alkyltrichlorosilanes and surfaces: Monomolecular and oligomeric covalently attached layers of dichloro- and trichloroalkylsilanes on silicon. *Langmuir*, *16*(18), 7268–7274.

Fuhrer, R., Athanassiou, E. K., Luechinger, N. A., & Stark, W. J. (2009). Crosslinking metal nanoparticles into the polymer backbone of hydrogels enables preparation of soft, magnetic field-driven actuators with muscle-like flexibility. *Small*, *5*(3), 383–388.

Guo, M., Ding, B., Li, X., Wang, X., Yu, J., & Wang, M. (2010). Amphiphobic nanofibrous silica mats with flexible and high-heat-resistant properties. *Journal of Physical Chemistry C*, *114*(2), 916–921.

Hozumi, A., Ushiyama, K., Sugimura, H., & Takai, O. (1999). Fluoroalkylsilane monolayers formed by chemical vapor surface modification on hydroxylated oxide surfaces. *Langmuir*, *15*(22), 7600–7604.

Hu, W. L., Chen, S. Y., Li, X., Shi, S. A. K., Shen, W., Zhang, X., et al. (2009). In situ synthesis of silver chloride nanoparticles into bacterial cellulose membranes. *Materials Science & Engineering C: Biomimetic and Supramolecular Systems*, *29*(4), 1216–1219.

Huang, H. C., Chen, L. C., Lin, S. B., & Chen, H. H. (2011). Nano-biomaterials application: In situ modification of bacterial cellulose structure by adding HPMC during fermentation. *Carbohydrate Polymers*, *83*(2), 979–987.

Jung, Y. C., & Bhushan, B. (2006). Contact angle, adhesion and friction properties of micro-and nanopatterned polymers for superhydrophobicity. *Nanotechnology*, *17*(19), 4970–4980.

Lafuma, A., & Quéré, D. (2003). Superhydrophobic states. *Nature Materials*, *2*(7), 457–460.

Leslie-Pelecky, D. L., & Rieke, R. D. (1996). Magnetic properties of nanostructured materials. *Chemistry of Materials*, *8*(8), 1770–1783.

Levison, P. R., Badger, S. E., Dennis, J., Hathi, P., Davies, M. J., Bruce, I. J., et al. (1998). Recent developments of magnetic beads for use in nucleic acid purification. *Journal of Chromatography A*, *816*(1), 107–111.

Li, X., Chen, S., Hu, W., Shi, S., Shen, W., Zhang, X., et al. (2009). In situ synthesis of CdS nanoparticles on bacterial cellulose nanofibers. *Carbohydrate Polymers*, *76*(4), 509–512.

Liang, Y. Y., Zhang, L. M., Jiang, W., & Li, W. (2007). Embedding magnetic nanoparticles into polysaccharide-based hydrogels for magnetically assisted bioseparation. *ChemPhysChem*, *8*(16), 2367–2372.

Luo, X., Liu, S., Zhou, J., & Zhang, L. (2009). In situ synthesis of Fe_3O_4/cellulose microspheres with magnetic-induced protein delivery. *Journal of Materials Chemistry*, *19*(21), 3538–3545.

Mackay, M. E., Tuteja, A., Duxbury, P. M., Hawker, C. J., Van Horn, B., Guan, Z., et al. (2006). General strategies for nanoparticle dispersion. *Science*, *311*(5768), 1740–1743.

Maneerung, T., Tokura, S., & Rujiravanit, R. (2008). Impregnation of silver nanoparticles into bacterial cellulose for antimicrobial wound dressing. *Carbohydrate Polymers*, *72*(1), 43–51.

Michael, N., & Bhushan, B. (2007). Hierarchical roughness makes superhydrophobic states stable. *Microelectronic Engineering*, *84*(3), 382–386.

Miwa, M., Nakajima, A., Fujishima, A., Hashimoto, K., & Watanabe, T. (2000). Effects of the surface roughness on sliding angles of water droplets on superhydrophobic surfaces. *Langmuir*, *16*(13), 5754–5760.

Pagliaro, M., & Ciriminna, R. (2005). New fluorinated functional materials. *Journal of Materials Chemistry*, *15*(47), 4981–4991.

Shim, I. W., Noh, W. T., Kwon, J., Cho, J. Y., Kim, K. S., & Kang, D. H. (2002). Preparation of copper nanoparticles in cellulose acetate polymer and the reaction chemistry of copper complexes in the polymer. *Bulletin of the Korean Chemical Society*, *23*(4), 563–566.

Small, A. C., & Johnston, J. H. (2009). Novel hybrid materials of magnetic nanoparticles and cellulose fibers. *Journal of Colloid and Interface Science*, *331*(1), 122–126.

Song, X., Zhai, J., Wang, Y., & Jiang, L. (2006). Self-assembly of amino-functionalized monolayers on silicon surfaces and preparation of superhydrophobic surfaces based on alkanoic acid dual layers and surface roughening. *Journal of Colloid and Interface Science*, *298*(1), 267–273.

Sourty, E., Ryan, D. H., & Marchessault, R. H. (1998). Characterization of magnetic membranes based on bacterial and man-made cellulose. *Cellulose*, *5*(1), 5–17.

Tang, H., Wang, H., & He, J. (2009). Superhydrophobic titania membranes of different adhesive forces fabricated by electrospinning. *Journal of Physical Chemistry C*, *113*(32), 14220–14224.

Tokoh, C., Takabe, K., Fujita, M., & Saiki, H. (1998). Cellulose synthesized by *Acetobacter xylinum* in the presence of acetyl glucomannan. *Cellulose*, *5*(4), 249–261.

Yano, H., Sugiyama, J., Nakagaito, A. N., Nogi, M., Matsuura, T., Hikita, M., et al. (2005). Optically transparent composites reinforced with networks of bacterial nanofibers. *Advanced Materials*, *17*(2), 153–155.

Zalich, M. A., Vadala, M. L., Riffle, J. S., Saunders, M., & St. Pierre, T. G. (2007). Structural and magnetic properties of cobalt nanoparticles encased in siliceous shells. *Chemistry of Materials*, *19*(26), 6597–6604.

Zhou, J. P., Li, R., Liu, S. L., Zhang, L. Z., Zhang, L. N., & Guan, I. G. (2009). Structure and magnetic properties of regenerated cellulose/Fe_3O_4 nanocomposite films. *Journal of Applied Polymer Science*, *111*(5), 2477–2484.

Zhu, Y., Tong, W., Gao, C., & Möhwald, H. (2008). Fabrication of bovine serum albumin microcapsules by desolvation and destroyable cross-linking. *Journal of Materials Chemistry*, *18*(10), 1153–1158.

Zhu, Y., Zhang, J. C., Zhai, J., Zheng, Y. M., Feng, L., & Jiang, L. (2006). Multifunctional carbon nanofibers with conductive, magnetic and superhydrophobic properties. *ChemPhysChem*, *7*(2), 336–341.

Zrínyi, M., Barsi, L., & Büki, A. (1997). Ferrogel: A new magneto-controlled elastic medium. *Polymer Gels and Networks*, *5*(5), 415–427.